Pulsations Along Stellar Evolution
VIII LAPIS Summer School
AAA Workshop Series 12, 2021
M. Kraus & A.F. Torres, eds.

Wavelets Analysis for Time Series

A. Christen[1]

[1] *Universidad de Valparaíso, Gran Bretaña 1111, 2340000 Valparaíso, Chile*

Abstract. Wavelet analysis has been widely used to analyze time series and has countless applications in astronomy. Because of its characteristics it is a method that is well suited to approximate functions, eliminate noise, detect points of change, discontinuities and periodicities. In this article an introduction to the wavelet theory and its use in time series is presented. Numerical simulations and some real examples are developed in the software R.

Key words: Methods: statistical — Methods: analytical — wavelets.

1. Introduction

Fourier transform is widely used in signal processing and analysis and for its inherent characteristics it has had satisfactory results in the study of signals that are periodic and regular enough, but the same is not true when their spectra vary over time (non-stationary signals). If the function $f(x)$ to be decomposed is a time series, and we think to analyze it, we have to take into account that the functions of the Fourier base are of infinite duration in time, but local in frequency. The Fourier Transform detects the presence of a certain frequency but does not provide information about the evolution in time of the spectral characteristics of the signal. Many temporal aspects of the signal, such as the beginning and end of a finite signal and the instant of appearance of a singularity in an instant of time, cannot be adequately analyzed by Fourier analysis. Even so, Fourier analysis is a cornerstone for the development of other mathematical and statistical theories including Wavelet analysis. In the following subsection we present the main concepts of Fourier analysis, which will be needed for the reading of the rest of the Chapter.

1.1. Some Concepts From Fourier Analysis

In this section we will review some concepts of Fourier analysis necessary for the following sections. Consider the space of all complex-valued functions f on R, such that f is absolutely integrable (ie: $\int_{-\infty}^{\infty}|f(x)|dx < \infty$) and denote it as $L^1(\mathrm{R})$ (Härdle et al. (1998)). For $f \in L^1(\mathrm{R})$, define the *Fourier Transform* of f by

$$\hat{f}(\xi) = \int_{-\infty}^{\infty} e^{-i\xi x} f(x)dx. \tag{1}$$

If $\hat{f}(\xi)$ is also absolutely integrable, define the *Inverse Fourier Transform* by

$$f(x) = \frac{1}{2\pi} \int_{-\infty}^{\infty} e^{i\xi x} \hat{f}(\xi) d\xi, \tag{2}$$

at almost every point x. By extension, the Fourier transform can be defined for any $f \in L^2(\mathrm{R})$ with $\int_{-\infty}^{\infty} |f(x)|^2 dx < \infty$.

Given a 2π-periodic function f on R, such that $f \in L^2(0, 2\pi)$ ($\int_0^{2\pi} |f(x)|^2 dx < \infty$), it can be represented by its Fourier series by

$$f(x) = \sum_k c_k e^{ikx}, \tag{3}$$

where $c_k = \frac{1}{2\pi} \int_0^{2\pi} f(t) e^{-ikx} dx$ is named the k-th Fourier coefficient. By periodicity, this holds for all $x \in \mathrm{R}$.

Therefore there exists the basis of functions, $\{e^{-ikx}\}_k$, in $L^2(\mathrm{R})$, for which we can write any function in $L^2(\mathrm{R})$ as an infinite linear combination of the members of this basis of functions. If we keep a finite number of terms on the right hand side of the equation (3), we will obtain an approximation of the function $f(x)$. Due to the characteristics of the Fourier series (the functions $\sin(x)$ and $\cos(x)$ in e^{-ikx} are non-zero over almost the entire domain), a large number of terms in the series are needed to get a good approximation of $f(x)$. In wavelet theory an alternative basis of functions is sought that has the property of being able to write any function in $L^2(\mathrm{R})$ as a series of the basis functions, but that they take values close to 0 outside a bounded interval, which allows a local adjustment in time and the use of few terms in the series to obtain a very good approximation of $f(x)$.

Let $\{a_k\}_{k \in \mathrm{Z}}$ denote an infinite sequence of real or complex-valued variables with the property that $\sum_{-\infty}^{\infty} |a_k|^2 < \infty$ what ensure that all the quantities we deal with are well defined. Then the complex function given by

$$A(r) = \sum_{k=-\infty}^{\infty} a_k e^{-i2\pi rk}, \tag{4}$$

is called the *Discrete Fourier Transform (DFT)* of $\{a_k\}_{k \in \mathrm{Z}}$, where $r \in \mathrm{R}$ is a variable known as *frequency* (see Percibal & Walden (2000)). For the interpretation of the formula in equation (4), $|r|$ is the number of cycles that the sinusoidal curves in the real and imaginary terms of the function $e^{-i2\pi rk} = cos(2\pi rk) - i\sin(2\pi rk)$ (i.e. $\cos(2\pi rk)$ and $-\sin(2\pi rk)$, respectively), go over when k sweeps from 0 to 1. Any negative frequency r will map to some positive frequency when a physical interpretation is required (see Percibal & Walden (2000), Exercise [2.1]).

As intuition, if $|A(r)|$ is large (small), then the sequences $\{a_k\}$ and $\{e^{-i2\pi rk}\}$ have a good agreement (bad agreement).

The sequence $\{a_k\}$ can be reconstructed or recovered from its DFT, $A(r)$, by

$$a_k = \int_{-\frac{1}{2}}^{\frac{1}{2}} A(r) e^{i2\pi rk} dr, \tag{5}$$

where $k \in \mathrm{Z}$. The larger the value of $|A(r)|$, the more important sinusoids of frequency r are in reconstructing $\{a_k\}$. If $\{a_k\}$ is a finite sequence for instance for $k = 1, \cdots, N$, it is extended to $k \in \mathrm{Z}$ by defining $a_k = 0$ for all $k \leq 0$ and $k > N$. In this case, $A(r) = \sum_{k=1}^{N} a_k e^{-i2\pi rk}$.

Filtering: In wavelets context it is often used the term "filter". Consider two infinite sequences of real or complex-valued variables, $\{a_k\}$ and $\{b_k\}$, satisfying $\sum_{k=-\infty}^{\infty} |a_k|^2 < \infty$, $\sum_{k=-\infty}^{\infty} |b_k|^2 < \infty$. The *convolution* of $\{a_k\}$ and $\{b_k\}$ is given by

$$(a * b)_k = \sum_{u=-\infty}^{\infty} a_u b_{k-u}. \tag{6}$$

This definition led us to the notion of filtering used in engineering. If we consider $\{a_k\}$ in equation (6) as a filter and $\{b_k\}$ as a sequence to be filtered, then their convolution, $\{(a*b)_k\}$, is the filtered version of $\{b_k\}$, filtered by the sequence $\{a_k\}$. There are 'low-pass' filters that preserve low frequency components and attenuate high frequency ones; and there are 'high-pass' filters that make the contrary. Finally there is a *cascade of filters*, involved in wavelet coefficients computation from data (see section 3), which is nothing more than the consecutive application of a set of filters to a sequence, one after the other.

1.2. Short Time Fourier Transform

An intermediate step between Fourier and Wavelet analysis was the use of the Short Time Fourier Transform (STFT) to detect local phenomena in time. It performs a time-dependent spectral analysis. The signal is divided into a sequence of time segments (depending on a window defined for this purpose) in which the signal can be considered as quasi-stationary and then the Fourier Transform is applied to each segment. Window functions are used to perform this procedure. To observe a signal over a finite period of time, we multiply it by a window function. The signal is divided into short fragments (short time intervals) delimited in time, by means of a window function. The segments sometimes overlap. Through the individual spectral analysis of each windowed segment, a sequence of measurements or spectra is obtained, what constitutes the time-varying spectrum. The four most common window types are the Rectangular window, the Hanning window, the Hamming window and the Blackman window.

Three kinds of examples where STFT has been applied are presented below: two curves with marked periodicities that change according to the time instant in Figure 1, two curves without periodicities in Figure 3 and one curve with variable periodicity in Figure 4.

Figure 1 shows the STFT of two sinusoidal curves, a curve with three different periods and amplitudes:

$$f_0(x) = \sin(0.2\pi x),\ f_1(x) = 1.5\sin(0.5\pi x),\ f_2(x) = 2\sin(0.8\pi x),$$

for the upper left panel, and

$$f_3(x) = \sin(0.6x),\ f_4(x) = 0.5\sin(0.5x),\ f_5(x) = 2\sin(0.1x),$$

for the lower left panel. In right panels of Figure 1 the computation of the corresponding STFT is shown. Time-slices of length 80 are extracted from the vector (in case of short vectors the window size is chosen so that 10 windows fit in the vector). The shift of one time-slice to the next one is given by 24 (for short vectors the increment is selected so that 30 increments fit in the vector). The values of these time-slices are smoothed by multiplying them with a Hanning window function. For these obtained windows, the Fast Fourier Transform[1] is computed. Then each window takes a segment of length 80 in time and is shifted by 24 which produces 414 calculations of the Fast Fourier transform. Therefore a matrix of 414 rows is produced where each row of the matrix contains the Fourier coefficients of one window which are plotted in a scale of 64 gray values, where white corresponds to the minimum value and black to the maximum. The right panel of the Figure 1 shows how the Fourier transform changes over time, which gives an indication of the change in periodicity over time. This is an advantage over the use of periodograms based on the Fourier transform in which the periods present are shown but without indicating their variability over time (see Figure 2 where the Lomb Scargle periodogram of the sine wave 1 is displayed). With wavelet analysis it will be possible to construct a time-sensitive measure, of the STFT type, where on the ordinate axis the exact time is shown.

In the Figure 3 two curves and their STFT are shown. On the left upper panel a Gaussian white noise is plotted. This curve is completely random with no periodicities, therefore no time with a specific value is highlighted in its STFT (right upper panel). On the left lower panel a sample of an Autoregressive Moving Average (ARMA) process with parameters $(2, 2)$ is shown. This is a linear model for time series analysis and together with Autoregressive Integrated Moving Average ARIMA and Continuous Autoregressive Moving Average CARMA models have been used to model light curves in astronomy (Cáceres (2019), Eyheramendy et al. (2018), Kelly et al. (2014)). The ARMA process is a stationary process with constant expectation and variance, so its representation contains no trend or periodicity. As a consequence, the STFT is less random than that of white Gaussian noise but with a time-varying Fourier transform. A curve with time-varying periodicity is plotted on the left panel of Figure 4. It can be seen that its STFT detects how the frequency decreases over time, although the exact time at which the changes occur or the exact trend of change is not visible due to the displacement of the windows used in the STFT calculation.

STFT allows that a certain location of a local phenomenon in a signal is detected. However, only the time interval in which the local phenomena occur will be known, since the location depends on the width of the window chosen. Moreover, the events will not be able to be differentiated or found if they are very close to each other, since it is not possible to distinguish different behaviors

[1]Fast Fourier Transform: Calculating the DFT is time consuming and requires on the order of N^2 floating point multiplications. As many of the multiplications are repeated by varying the indexes, an efficient algorithm is used, called Fast Fourier Transform (FFT) which consists of a collection of routines designed to reduce the amount of redundant calculations. Different implementations of the FFT have different features and advantages. One of the algorithms used is the "split-radix" algorithm which requires approximately $N \log_2(N)$ operations (Fischer-Cripps (2002)).

within the same window width. A mathematical tool to solve these problems is the Wavelet Transform.

In this Chapter, the theory of Wavelet analysis is described in Section 2 including multiresolution analysis. Section 3 describes the Cascade Algorithm and the discrete wavelet transform while Section 4 is devoted to continuous wavelet transform and its applications. Finally, in Section 5 we present our conclusions.

2. Theory of Wavelet Analysis

We can say that the theory of the analysis of the wavelets began with Mr. Joseph Fourier (1807), with his theory of frequency analysis, today often referred to as Fourier analysis. After 1807 and from the development of the Fourier convergent and orthogonal systems, the notion of frequency analysis led to scale analysis. The first mention of the wavelets appears in an appendix of the thesis of A. Haar (1909). The wavelet theory was developed mainly in the 80's by Meyer (1986), Daubechies (1988), Mallat (1989) and others.

Wavelets are used in a large number of applications, among them: astronomy, acoustics, nuclear engineering, sub-band code, signal and image processing, neurophysiology, bioinformatics, genetics, music, magnetic resonance imaging, classification of words in a text, optics, fractals, seismic turbulence prediction, radars, human vision, statistics (time series, correlations, stochastic processes, point processes, non-parametric regression, regression with census data) and mathematical applications such as: in pure frequency identification, eliminating signal noise, detecting discontinuities and cutting spots, detecting self-similarity (fractals), compression of data.

In this Chapter the use of wavelets focuses on their application to time series (i.e.: sequence of observations indexed on an ordered set of indices I which can be a discrete set of values such as integers or a subset of the real line, based on an independent variable $t \in I$). The variable t can be taken as time, depth, or distance along a line, among others. Examples of set of indexes are $I = (0, +\infty)$, that is, all $t > 0$ are possible indexes, and $I = \{0, 1, 2, \cdots, n\}$, where n can be any integer greater than 2.

The main points of the theory of wavelet analysis are developed to later analyze its use in applications through approximations, scalograms built from the wavelet transform, signal reconstruction, among others. The Wavelet Transform is efficient for the local analysis of locally changing and non-stationary signals and, like the Windowed Fourier Transform[2], assigns a time-scale representation to the signal. The time aspect of the signals is under consideration. The main difference with STFT is that the Transformed Wavelet has multiresolution analysis with variable windows. The analysis of higher range frequencies is done using narrow windows and the analysis of lower range frequencies is done using wide windows (Poularikas, 2010).

[2]Short Time Fourier Transform

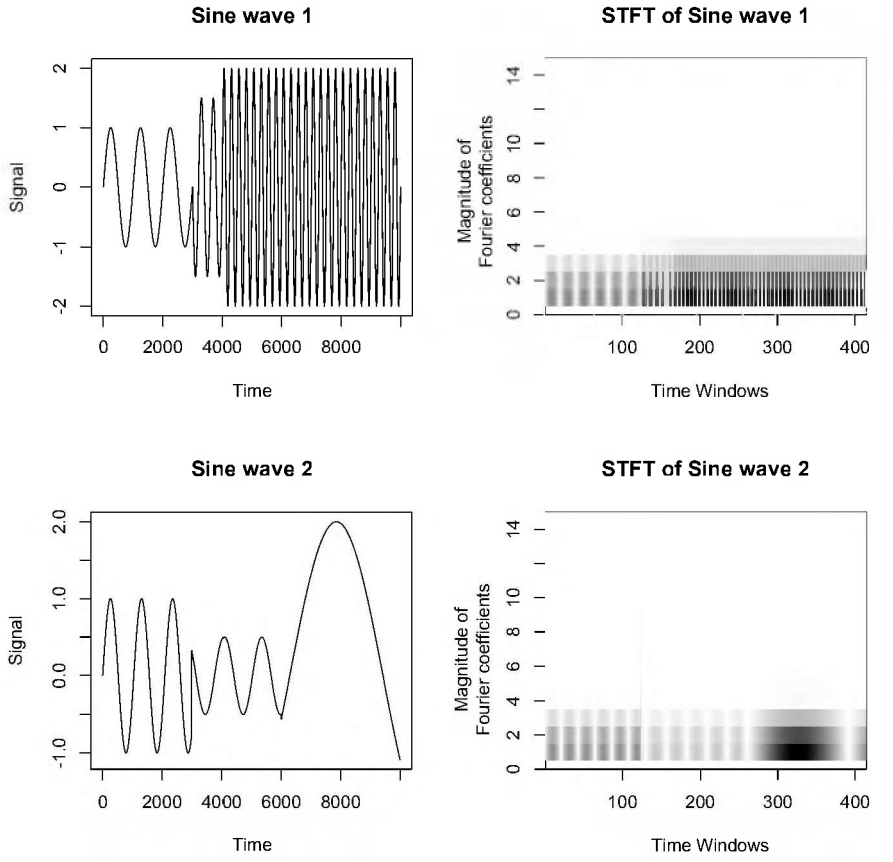

Figure 1. Examples of STFT. On the left panels, it can be seen two different sinusoidal curves and on the right panels their STFT. First, time segments of a fixed length are extracted from the data vector. This window is moved along the time axis by a fixed amount possibly smaller than the window size, which may produce an overlap between the time segments. The values of these time intervals are smoothed by multiplying them by a specified window function. For the windows thus obtained, the fast Fourier transform is calculated. For the data in the figure, segments of 80 time units were used. They were incremented by 24 units to obtain the next segment, which produced overlapping segments, yielding 414 windows. For each window 64 Fourier coefficients were calculated. The figure shows: on the x-axis the 414 windows and 64 cells on the vertical axis of each window which were colored with a gray scale according to the magnitude of the Fourier coefficients. In the figure only the cells with gray colors are observed, the rest are only white. The dark regions in the graph correspond to high values of the coefficients at the particular time/frequency location.

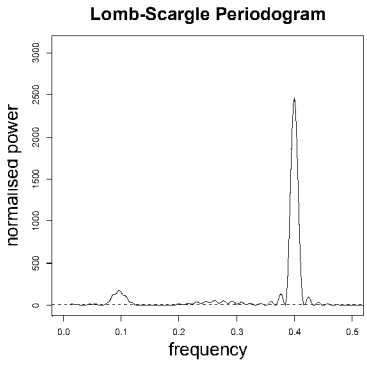

Figure 2. In the figure the Lomb Scargle periodogram of Sine wave 1 is shown. The frequencies of the curve 0.1 and 0.4 are clearly evidenced and more weakly the frequency 0.25.

Wavelets (small waves) are families of functions which, if they are translated and dilated, allow us to obtain an orthogonal base of functions in $L^2(\mathrm{R})$. A linear combination of the elements of this base of wavelet functions is used to represent a signal $f(t)$.

The classical Fourier analysis has been widely used in the problem of reconstructing a function f from dilations of a fixed sinusoidal function $x \mapsto e^{2\pi i x}$, when writing $f(x) = \int e^{2\pi i \xi x} \hat{f}(\xi) d\xi$. The Fourier transform, $\hat{f}(\xi)$, is considered the amount of sinusoidal oscillation $e^{2\pi i \xi x}$ present in the function f. Sinusoidal function bases are also used in Fourier series.

In the same way the wavelet basis of functions allows us to reconstruct the original signal through the inverse Wavelet Transform. There are several base wavelet functions, depending on the chosen family: Haar, Daubechies, Morlet, Symmlets, among others. Depending on the selected wavelet family, a different base function is used (first brick in the construction) and a certain base of functions is obtained which will allow the wavelet analysis to be performed. The main advantage of Wavelet analysis is that it is not only local in time, but also in frequency.

This feature allows using the continuous wavelet transform to detect an event in the data, either the period of a time series, a change point in the series, a discontinuity in a density function, and to know the moment (time) or abscissa at which it occurs. For example, knowing the time interval during which a detected period is present in the brightness measurements in a light curve, the moment when the flow of a river changes drastically, the day when an economic variable produces a change in its modeling.

Another feature of a wavelet functions basis is that any function in the function space L^2 can be decomposed as an infinite sum of functions in the wavelet basis, as with the Fourier series, but because of their great flexibility to approximate functions efficiently only a small number of summands are needed to produce very good approximations. The latter is because wavelet functions vanish outside a bounded interval and the basis of functions is formed by a count-

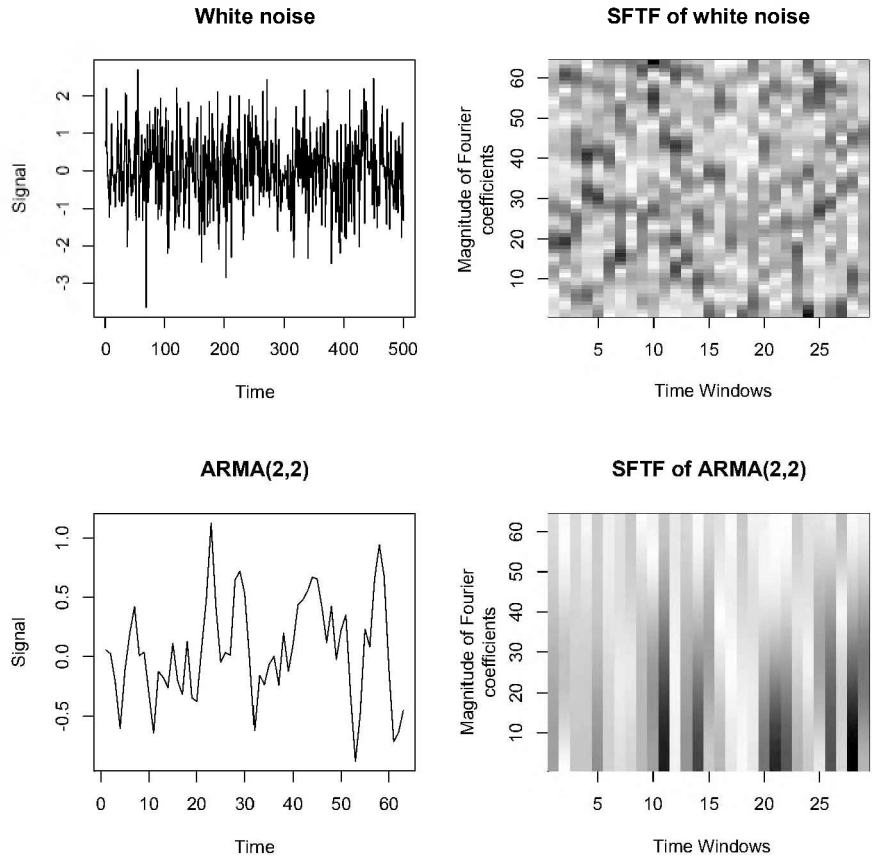

Figure 3. Examples of STFT: The upper panel shows a curve of 500 data points from a Gaussian white noise and its STFT. In the lower panel, the plots show the curve of a sample from an ARMA $(2, 2)$ process and its STFT. For the data in the upper right panel of the figure, segments of 50 time units were used. They were incremented by 16 units to obtain the next segment, which produced overlapping segments, yielding 29 windows. For each window 64 Fourier coefficients were calculated. The figure shows: on the x-axis the 29 windows and 64 cells on the vertical axis of each window which were colored with a gray scale according to the magnitude of the Fourier coefficients. The dark regions in the graph correspond to high values of the coefficients at the particular time/frequency location. In the lower right panel, segments of 6 time units with increments of 2 units were used, yielding 29 windows.

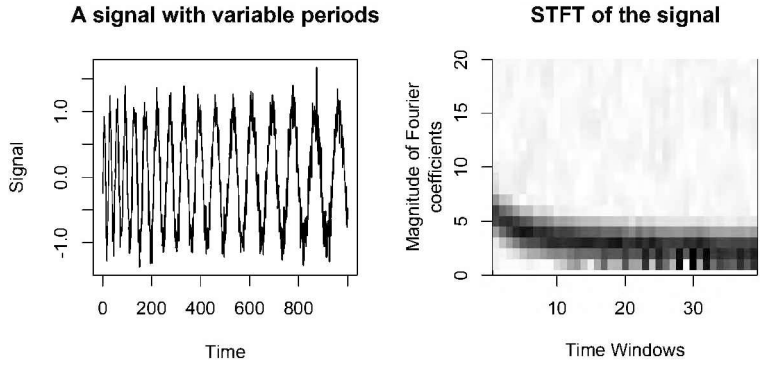

Figure 4. On the left panel, it can be seen a curve with periods varying over time and on the right panel its STFT, built from segments of 80 time units with increments of 24 units, yielding 39 windows on the x-axis. On the vertical axis of each window 64 cells were colored with a gray scale according to the magnitude of the Fourier coefficients. In this figure the dark regions, corresponding to a high magnitude of the Fourier coefficient, sweep across an interval as they move through time.

able number of dilations and contractions of a wavelet function called "parent", stretches and squashes of those functions and translations of all of them. This is equivalent to having bricks of various sizes and widths that can be placed under any house and that adding up all the volumes will give exactly the same volume of the house.

In the next section we will be introduced to multiresolution analysis, the main feature of wavelet analysis, which will allow us to define a basis of wavelet functions in $L^2(\mathrm{R})$ with which we can represent any function $f(x)$ in $L^2(\mathrm{R})$ through an infinite countable linear combination of the basis.

2.1. Multiresolution Analysis

Wavelets can be considered as a basis of functions generated by dilations and translations of a simple function which, in general, is not sinusoidal. They are connected to the notion of multiresolution analysis (MRA) in which the objects (signals, functions, data) can be examined using several levels of approach, as if zooming in and out. In both cases we can obtain relevant information about the object. As an example, suppose we are looking at a house, the observation can be made from a large distance from where only the basic shapes and structure can be distinguished (if it has a garage, the shape of the roof); or one can observe from a closer distance and various other characteristics of the house will appear (the door is made of hardwood, for example).

The basis function will be generated from a basic function that is usually called parent wavelet or scaling function, which in turn allows us to build another basic function that we will call mother wavelet or wavelet function. The repre-

sentation of a function $f(x)$ will be done through two summands: the sum of the dilations and translations of the father wavelet, $\varphi(x)$, will give us information about the general, coarse aspects (a kind of smoothing) of the $f(x)$ and the sum of the dilations and translations of the mother wavelet, $\psi(x)$, will give us information about the particular aspects and details (like a zoom) of the function. Each term in the second summand will add more clarity on the specific features.

In this section some basic concepts such as wavelet father, which provides smoothing, and wavelet mother, to describe the details, are defined to reach the multiresolution analysis definition. In the following it will be assumed that the function to be analyzed is a function of time t.
For $\varphi \in L^2(\mathrm{R})$, $k \in \mathrm{Z}$, $x \in \mathrm{R}$, we denote $\varphi_{0k}(x) = \varphi(x-k)$ the family of translations of φ and we denote

$$\varphi_{jk}(x) = 2^{\frac{j}{2}}\varphi(2^j x - k), j, k \in \mathrm{Z},$$

the family of translations and dilations of φ with the indexes k and j respectively. The functional sub-spaces $\{V_j\}_{j\in\mathrm{Z}}$, $V_j \subseteq L^2(\mathrm{R})$ are defined by:

- for $j = 0$:

$$V_0 = \left\{ g \in L^2(\mathrm{R}) : g(x) = \sum_k c_k \varphi(x-k),\ \sum_k |c_k|^2 < +\infty \right\}$$

  that is, V_0 is the subspace spanned by the translations of $\varphi(x)$ by k, $\varphi(x-k)$.

- and for $j \in \mathrm{Z}$:

$$V_j = \left\{ h(x) = g(2^j x) : g \in V_0 \right\}.$$

  Then $h(x) \in V_{j_1}$ if $h(x) = \sum_k c_k \varphi(2^{j_1}x - k)$ for $\{c_k\}$ such that $\sum_k |c_k|^2 < +\infty$, or, V_{j_1} is the subspace spanned by the functions $\{\varphi(2^{j_1}x-k)\}_{k\in\mathrm{Z}}$.

Therefore φ generates the sequence of subspaces $\{V_j\}$. The sequence $\{V_j\}$ is called *multiresolution analysis* if

1. $\{\varphi_{0k}\}$ is an ortonormal system in $L^2(\mathrm{R})$,
2. the subspaces are nested, that is,

$$V_j \subset V_{j+1}, j \in \mathrm{Z}, \tag{7}$$

3. every function in $L^2(\mathrm{R})$ can be obtained as a limit of a sequence of functions in $\bigcup_{j\geq 0} V_j$, that is, every function $f \in L^2(\mathrm{R})$ can be written as a series of elements in $\bigcup_{j\geq 0} V_j$.

In this case, φ is called *Wavelet father*. Another sequence $\{W_j\}_{j\in\mathrm{N_0}}$ is considered such that W_j is the orthogonal complement of $V_j \subseteq V_{j+1}$, $W_j =$

$V_{j+1} \ominus V_j$, then $\bigcup_{j\geq 0} V_j = V_0 \cup (V_1 \ominus V_0) \cup (V_2 \ominus V_1) \cdots \cup (V_{j+1} \ominus V_j) \cdots$. Then $\bigcup_{j\geq 0} V_j = V_0 \oplus \overset{\infty}{\underset{j=0}{\oplus}} (V_{j+1} \ominus V_j)$ is a direct sum of sub-spaces that completes $L^2(\mathrm{R})$ leading to

$$L^2(\mathrm{R}) = V_0 \oplus \overset{\infty}{\underset{j=0}{\oplus}} W_j,$$

therefore any function $f(x)$ in $L^2(\mathrm{R})$ can be written as a linear combination of functions in V_0 and $\{W_j\}$. For each $j \in \mathrm{N}_0$, let ψ be a function such that its translations and dilations, $\{\psi_{jk} = 2^{j/2}\psi(2^j x - k), k \in \mathrm{Z}\}$, are an orthogonal basis of W_j. Then, for instance, the translations $\{\psi_{0k}(x) = \psi(x-k)\}_k$ is an orthogonal system of W_0, this system is orthogonal to V_0 and $V_1 = V_0 \oplus W_0$ is the subspace spanned by the system $\{\{\varphi_{0m}\}_m, \{\psi_{0k}\}_k\}$, where $\varphi_{0m}(x) = \varphi(x-m)$ for all m.

As a consequence, each function $f(x)$ can be represented as a convergent series given by

$$f(x) = \sum_{k\in \mathrm{Z}} \alpha_k \varphi_{0k}(x) + \sum_{j=0}^{\infty} \sum_{k\in \mathrm{Z}} \beta_{jk}\psi_{jk}(x), \tag{8}$$

where

$$\alpha_k = \int f(x)\varphi_{0k}(x)dx, \quad \beta_{jk} = \int f(x)\psi_{jk}(x)dx. \tag{9}$$

According to the function $f(x)$ sometimes it is necessary to start with a subspace V_{j_0} with $j_0 > 0$, in that case, the first function in the sum, $\varphi_{0k}(x)$, is replaced by $\varphi_{j_0 k}(x)$ and the index j starts at $j_0 > 0$ in the right term of equation (8).

The representation of $f(x)$ as an expansion of translations and dilations of functions φ and ψ is called *wavelet expansion* and ψ the *Wavelet mother.*

Each W_j in the sequence of sub-spaces $\{W_j\}$ represents a *resolution level* of the multiresolution analysis. There are several levels j of resolution, what gives rise to its name.

The resolution level means a zoom level that is performed on the function, so each one will allow you to see details at different scopes. Thus the function is decomposed into an initial smoothing, given by the parent wavelet in the first term of the right-hand side of eq. (8) and different levels of details that are added according to the value of the level j in the second term of the right side. The greater the value of j, the greater the level of resolution and the finest details will be visible, which will be represented by the j-th term.

An example of wavelet system is the Haar system. The wavelet father and wavelet mother are given by

$$\varphi(x) = I_{(0,1]}(x), \quad \psi(x) = -I_{[0,\frac{1}{2}]}(x) + I_{(\frac{1}{2},1]}(x), \tag{10}$$

respectively, where

$$I_A(x) = \begin{cases} 1 & if\ x \in A \\ 0 & if\ x \notin A \end{cases}$$

and the interval $(a, b]$ is the set of real numbers between a and b, including b but not a. The basis of functions for the Haar wavelet system are:

$$\varphi_{0k}(x) = \{I_{(0,1]}(x-k)\}_{k\in \mathrm{Z}},$$

$$\psi_{jk}(x) = 2^{j/2}\left(I_{\left(\frac{1}{2},1\right]}\left(2^j x-k\right) - I_{[0,\frac{1}{2}]}(2^j x-k)\right),$$

for wavelet father and mother respectively, where $j, k \in \mathrm{Z}$, $j \geq 0$. We can observe that $\{\varphi_{0k}(x)\}_{k\in \mathrm{Z}}$ is an orthonormal basis (ONB, i.e.: a basis of orthogonal and normalized vectors) in

$$V_0 = \{h(x) \in L^2(\mathrm{R}) : h(x) \text{is constant on } (k, k+1], k \in \mathrm{Z}\},$$

$\{\varphi_{jk}(x) = 2^{j/2}\varphi(2^j x-k)\}_{k\in \mathrm{Z}}$ is an ONB in

$$V_j = \{h(x) \in L^2(\mathrm{R}) : h(x) = g(2^j x), g(x) \in V_0\},$$

$V_j \subseteq V_{j+1}$ and $V_j = V_{j-1} \oplus W_{j-1}$, where W_j is spanned by $\{\psi_{jk}(x)\}_{k\in \mathrm{Z}}$. Finally, $L^2(\mathrm{R}) = V_0 \oplus W_0 \oplus W_1 \oplus \cdots W_j \oplus \cdots$.

By way of illustration,

1. $\{\varphi_{0k}(x)\}$ is an ONB of V_0.

2. $V_1 = \{h(x) \in L^2(\mathrm{R}) : h(x) = g(2x), g(x) \in V_0\} = \{h(x) \in L^2(\mathrm{R}) : h(x) \text{is constant on } (\frac{k}{2}, \frac{k+1}{2}], k \in \mathrm{Z}\}$ and it is spanned by the ONB $\{\varphi_{0k}(x), \psi_{0k}(x) = I_{[0,\frac{1}{2}]}(x-k) - I_{\left(\frac{1}{2},1\right]}(x-k)\}$.

3. The functions $\varphi_{1k}(x) = 2^{1/2}\varphi(2x-k)$ for $k \in \mathrm{Z}$ span V_1 and can be written in terms of $\{\varphi_{0k}(x)\}$ and $\{\psi_{0k}(x)\}$, since $V_1 = V_0 \oplus W_0$. For instance:

$$\varphi_{10}(x) = \sqrt{2}I_{(0,\frac{1}{2}]}(x) = \frac{\sqrt{2}}{2}(I_{(0,1]}(x) - I_{[0,\frac{1}{2}]}(x) + I_{\left(\frac{1}{2},1\right]}(x)) = \frac{1}{\sqrt{2}}(\varphi_{00} - \psi_{00}),$$

$$\varphi_{11}(x) = \sqrt{2}I_{(0,1]}(2x-1) = \frac{1}{\sqrt{2}}(\varphi_{00} + \psi_{00}).$$

A suitable property of the Haar wavelets is that they are cancelled out of a limited interval. Unfortunately, Haar wavelets are not continuously differentiable which limits their applications (see Figure 5). There are wavelet families with compact support (vanish out of an interval) and wavelet families defined over the whole line. Among the former wavelet families are Daubechies, Coiflets, Symmlets. Some examples of the last ones are the Battle-Lemarié and Morlet wavelets.

Father and mother wavelets can be defined from some of the properties of their Fourier transforms (see Härdle et al. (1998)).

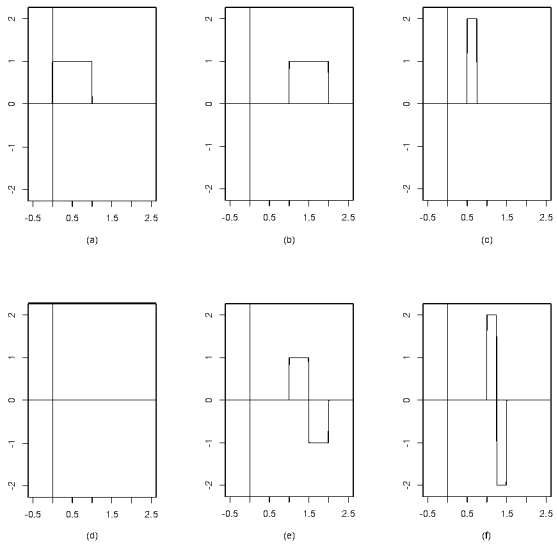

Figure 5. Some representations of Haar wavelet. On the top panel it is shown Haar father wavelet for (a) $j = 0$, $k = 0$, (b) $j = 0$, $k = 1$, (c) $j = 1$, $k = 1/2$. On the bottom panel it is shown Haar mother wavelet for (d) $j = 0$, $k = 0$, (e) $j = 0$, $k = 1$, (c) $j = 1$, $k = 1$.

2.2. Obtaining a Wavelet Expansion

In this section the conditions about functions φ and ψ that guarantee the existence of a wavelet system are formulated. That is to say, what characteristics should have so that φ_{0k} is an orthogonal and normalized system, the V_j are nested, the span of $\bigcup_j V_j$ is equal to $L^2(\mathrm{R})$, ψ_{jk} is an orthogonal and normalized system of W_j, etc. This section follows closely Härdle et al. (1998).

Properties on $\hat{\varphi}$, the Fourier transform of φ, are sought that guarantee the validity of the necessary and sufficient conditions for the wavelet expansion:

1. $\{\varphi_{0k}, k \in \mathrm{Z}\}$ is an orthonormal system (ONS)
2. $V_j \subset V_{j+1}, j \in \mathrm{Z}$
3. $\bigcup_{j\geq 0} V_j$ is dense in $L^2(\mathrm{R})$ (i.e.: the linear combinations of functions in $\bigcup_{j\geq 0} V_j$ span all the functional space $L^2(\mathrm{R})$).
4. $\{\psi(x-k), k \in \mathrm{Z}\}$ is an ONB in W_0.

In what follows functions φ, that satisfy that there is a constant $M > 0$ such that $\sum_{k\in\mathrm{Z}} |\varphi(x-k)| < M$ for $x \in \mathrm{R} - A$, will be considered, where A is a null measurement set.

The following results that allow characterizing the father wavelet and the mother wavelet from properties of their Fourier transform can be demonstrated (see Härdle et al. (1998)).

(a) Set $\varphi \in L^2(\mathrm{R})$. The system $\{\varphi_{0k}, k \in \mathrm{Z}\} = \{\varphi(x-k), k \in \mathrm{Z}\}$ is an ONS if and only if,

$$\sum_{k \in \mathrm{Z}} |\hat{\varphi}(\xi + 2\pi k)|^2 = 1, \tag{11}$$

almost everywhere (a.e.), where $\hat{\varphi}$ is the Fourier transform of the function φ.

(b) The sub-spaces $\{V_j, j \in \mathrm{Z}\}$, spanned by translations and dilations of φ, are nested $V_j \subset V_{j+1}, j \in \mathrm{Z}$, if and only if, there exists a 2π - periodic function $m_0 \in L^2(0, 2\pi)$ such that

$$\hat{\varphi}(\xi) = m_0\left(\frac{\xi}{2}\right)\hat{\varphi}\left(\frac{\xi}{2}\right), \ a.e. \tag{12}$$

Moreover, $|m_0(\xi)|^2 + |m_0(\xi+\pi)|^2 = 1$ a.e.

(c) If φ satisfies items (a) and (b) above then $\bigcup_{j \geq 0} V_j$ is dense in $L^2(\mathrm{R})$.

(d) If φ is a father wavelet that generates a MRA in $L^2(\mathrm{R})$, $m_0(\xi)$ is a solution of equation (12) then

$$\hat{\psi}(\xi) = m_1\left(\frac{\xi}{2}\right)\hat{\varphi}\left(\frac{\xi}{2}\right) \tag{13}$$

is the Fourier transform of a mother wavelet ψ, where $m_1(\xi) = \overline{m_0(\xi+\pi)}e^{-i\xi}$ and the bar represents the complex conjugate.

In summary, to construct a father wavelet φ for a MRA, sufficient conditions on its Fourier transform $\hat{\varphi}$ should satisfy the following restrictions:

$$\sum_{k \in \mathrm{Z}} |\hat{\varphi}(\xi + 2\pi k)|^2 = 1, \ a.e.,$$

$$\hat{\varphi}(\xi) = m_0\left(\frac{\xi}{2}\right)\hat{\varphi}\left(\frac{\xi}{2}\right),$$

where $m_0 \in L^2(0, 2\pi)$ is a periodic function of period 2π such that

$$\begin{cases} |m_0(\xi)|^2 + |m_0(\xi+\pi)|^2 = 1, \\ m_0(0) = 1, \end{cases} \tag{14}$$

where the last restriction in equation (14) is deduced of eq. (12) after adding the condition $|\hat{\varphi}(0)| = |\int \varphi(t)dt| = 1$ for the father wavelet.

Since $V_0 \subset V_1$, then $\varphi \in V_1$ and it can be written as a linear combination of the system $\{\sqrt{2}\varphi(2x-k)\}$, an ONB of the subspace V_1. Therefore, there is a sequence $\{h_k\}$ such that

$$\varphi(x) = \sqrt{2}\sum_{k\in \mathrm{Z}} h_k \varphi(2x-k), \quad h_k = \sqrt{2}\int \varphi(x)\varphi(2x-k)dx, \tag{15}$$

with $\sum_{k\in \mathrm{Z}} |h_k|^2 < \infty$ and the constraints

1. $\sum_k \overline{h_k} h_{k+2l} = \delta_{0l}$
2. $\frac{1}{\sqrt{2}}\sum_k h_k = 1.$

where $\delta_{0l} = 0$ if $l \neq 0$ and $\delta_{0l} = 1$ if $l = 0$. By the same argument the mother wavelet satisfies

$$\psi(x) = \sqrt{2}\sum_k \lambda_k \varphi(2x-k), \tag{16}$$

where $\lambda_k = (-1)^{k+1}\overline{h_{1-k}}$.

Taking Fourier transform to both sides of left equation in (15) we obtain $\hat{\varphi} = \frac{1}{\sqrt{2}}\sum_k h_k e^{-i\xi k}\frac{\hat{\varphi}}{2}$ and by eq. (12) we have that

$$m_0(\xi) = \frac{1}{\sqrt{2}}\sum_k h_k e^{-i\xi k}. \tag{17}$$

If the wavelets considered are compactly supported (i.e.: they vanish outside a bounded interval), the sums in eqs. (15), (16) and (17) have a non-zero number of terms. These relations allow us to determine the coefficients in eq. (9) of a function in its wavelet representation in eq. (8) through a linear transformation given by the product of a matrix by a vector.

Compactly supported wavelets

Some of the wavelet families with compact support are the Daubechies, Coiflets and Symmlets. We briefly describe each of them.
Ingrid Daubechies, to whom we owe the original construction of Wavelets with compact support (Daubechies (1988)), proposed to take $m_0(\xi)$ such that

$$|m_0(\xi)|^2 = c_N \int_\xi^\pi \sin^{2N-1}(x)dx, \tag{18}$$

where the constant c_N is chosen to produce $m_0(0) = 1$. For such functions $m_0(\xi)$ the coefficients $\{h_k\}$ are tabulated (see Daubechies (1988) or Härdle et al. (1998)). Wavelets constructed from the function $m_0(\xi)$ satisfying eq. (18) are called *Daubechies Wavelets* and they are denoted $D2N$ or $Db2N$.

For $N = 1$, we have $D2$ where $c_N = \frac{1}{2}$ and

$$|m_0(\xi)|^2 = \frac{1}{2}\int_{\xi}^{\pi} \sin(x)dx = \frac{1 + cos(\xi)}{2}.$$

Choosing $m_0(\xi) = \frac{1+e^{-i\xi}}{2}$ we obtain

$$\hat{\varphi}(\xi) = \lim_{n\to\infty} \prod_{j=1}^{n} \frac{1}{2}(1 + e^{-\frac{i\xi}{2^j}}) = \frac{1 - e^{-i\xi}}{i\xi},$$

hence Daubechies father wavelet $D2$ matches with Haar father wavelet, $\varphi(x) = I\{x \in (0, 1]\}$.

The supports of Daubechies father wavelet and mother wavelet are included in the intervals $[0, 2N - 1]$ and $[-N + 1, N]$, respectively. Besides, Daubechies mother wavelet has null m-moment (i.e.: $\int x^m \psi(x)\, dx = 0$) for $m = 0, ..., N - 1$.

Beylkin et al. (1991) proposed a new class of wavelets with essentially the same good properties of the Daubechies wavelets and, in addition, the father wavelet has some zero moments. If the father wavelet has certain null moments the wavelet coefficients could be approximated by evaluations of the function $f(t)$ at discrete points:

$$\alpha_{jk} = 2^{-j/2} f\left(\frac{k}{2^j}\right) + r_{jk},$$

with r_{jk} small enough. This can be a useful property in applications.

This class of wavelets was called *Coiflets Wavelets* and is denoted CK. To build the Coiflets wavelets, Beylkin et al. (1991) consider $m_0(\xi)$ of the form

$$m_0(\xi) = \left(\frac{1 + e^{-i\xi}}{2}\right)^{2K} P_1(\xi),$$

where

$$P_1(\xi) = \sum_{k=0}^{K-1} C_{K-1+k}^{k} \left(\sin^2\left(\frac{\xi}{2}\right)\right)^k + \left(\sin^2\left(\frac{\xi}{2}\right)\right)^K F(\xi),$$

and $F(\xi)$ is a trigonometric polynomial chosen such that $|m_0(\xi)|^2 + |m_0(\xi + \pi)|^2 = 1$. The supports of Coiflets father wavelet and mother wavelet are included in the intervals $[-2K, 4K - 1]$ and $[-4K + 1, 2K]$, respectively.

According to Daubechies (1992) the only symmetric wavelet with compact support is the Haar system (father wavelet). The family of *Symmlet Wavelets* is made up of wavelets for which $m_0(\xi)$ is chosen to be close to symmetry. They are denoted by SN, where N is the order of the wavelet. Symmlet mother wavelet has null m-moment (i.e.: $\int x^m \psi(x)\, dx = 0$) for $m = 0, ..., N - 1$. The support of the father wavelet and mother wavelet are the intervals given by $[0, 2N - 1]$ and $[-N + 1, N]$, respectively.

3. Cascade Algorithm

Some recursive formulas are presented that will allow the calculation of the wavelet coefficients sequentially (see Härdle et al. (1998)). The procedure is called **Cascade algorithm** (or pyramidal). It was proposed by Mallat (1989).

This method (Härdle et al. (1998)) is used only with wavelet bases that vanish outside a finite interval and built from the function $m_0(\xi) = \frac{1}{\sqrt{2}} \sum_k h_k e^{-ik\xi}$ (see eq. (17)) where h_k are coefficients of real values with only a finite number of non-zero values. This assumption is satisfied by the families of Daubechies, Coiflets and Symmlets wavelets, among others.

Given a function $f(t)$, the coefficients $\alpha_{jk} =< f, \varphi_{jk} >$, $\beta_{jk} =< f, \psi_{jk} >$ satisfy for $j, k \in \mathrm{Z}$ the relationships:

$$\alpha_{jk} = \sum_k h_{l-2k} \alpha_{j+1,l}, \tag{19}$$

$$\beta_{jk} = \sum_k \lambda_{l-2k} \alpha_{j+1,l} \tag{20}$$

where $\lambda_k = (-1)^{k+1} h_{1-k}$ and $\{h_k\}$ are the coefficients of $m_0(\xi)$.

Indeed, by multiresolution analysis,

$$\begin{aligned}
\beta_{jk} &= 2^{\frac{j}{2}} \int f(x)\psi(2^j x - k)dx \\
&= 2^{\frac{j+1}{2}} \sum_s \lambda_s \int f(x)\varphi(2(2^j x - k) - s)dx \\
&= 2^{\frac{j+1}{2}} \sum_s \lambda_s \int f(x)\varphi(2^{j+1} x - 2k - s)dx \\
&= \sum_s \lambda_s \alpha_{j+1,s+2k} = \sum_l \lambda_{l-2k} \alpha_{j+1,l}.
\end{aligned}$$

The relation (19) is obtained in a similar way. The cascade algorithm is defined by both equations (19) and (20).

Only a finite number of coefficients α_{jk} are non-zero in each level j. Therefore if the vector of coefficients, $y = \{\alpha_{j_1 l}\}$ is known for a certain level j_1, it is possible to recursively rebuild the coefficients α_{jk}, β_{jk} for levels $j \leq j_1$, with the use of the recursive equations (19) and (20).

If the procedure stops at level j_0, the vector of resulting wavelets coefficients $w = (\{\alpha_{j_0 k}\}, \{\beta_{j_0 k}\}, ..., \{\beta_{j_1 - 1,k}\})^t$ can be computed by

$$w = \mathcal{W} y, \tag{21}$$

where $\mathcal{W}$ is a matrix.

It is possible to invert the cascade algorithm to obtain the values of the coefficients y, starting from w by the recursive scheme:

$$\alpha_{j+1,s} = \sum_k h_{s-2k}\alpha_{j,k} + \sum_k \lambda_{s-2k}\beta_{j,k}, \tag{22}$$

allowing j to vary from j_0 to $j_1 - 1$.

3.1. Discrete Wavelet Transform

Given the initial values $\{\alpha(K,k), k = 0, ..., 2^K - 1\}$ the *Discrete Wavelet Transform* (DWT) recursively calculates the coefficients $\alpha(j,k)$ and $\beta(j,k)$ for $0 \leq k \leq 2^j - 1$ and $0 \leq j \leq K - 1$, in the following manner:

$$\alpha(j,k) = \sum_l h_l\, \alpha(j+1, (l+2k)\ mod\ 2^{j+1}), \tag{23}$$

$$\beta(j,k) = \sum_l \lambda_l\, \alpha(j+1, (l+2k)\ mod\ 2^{j+1}). \tag{24}$$

where $(l+2k)\ mod\ 2^{j+1}$ denotes[3] the remainder of dividing $(l+2k)$ by 2^{j+1}. Therefore the DWT is just a composition of linear orthogonal transformations presented by the recursions (23) and (24). These recursions can be extended to $k \in$ Z and these extensions are periodic, in the sense that $\alpha(j,k) = \alpha(j, k + 2^j)$, $\beta(j,k) = \beta(j, k + 2^j)$ for all $k \in$ Z.

The Discrete Inverse Wavelet Transform is defined in a similar way but with the data periodically extended. It starts with the vectors:

$$\{\alpha(j_0,k), k = 0, ..., 2^{j_0} - 1\},\ \{\beta(j_0,k), k = 0, ..., 2^{j_0} - 1\}$$

and its periodic extensions are denoted by $\{\widetilde{\alpha}(j_0,k), k \in Z\}$, $\{\widetilde{\beta}(j_0,k), k \in Z\}$.

Then the vectors $\{\alpha(j,s), s = 0, ..., 2^j - 1\}$ are computed until level $j = K - 1$, following the recursive equations:

$$\widetilde{\alpha}(j+1,s) = \sum_k h_{s-2k}\ \widetilde{\alpha}(j,k) + \sum_k \lambda_{s-2k}\ \widetilde{\beta}(j,k), s \in Z, \tag{25}$$

$$\alpha(j+1,s) = \widetilde{\alpha}(j+1,s), s = 0, ..., 2^{j+1} - 1. \tag{26}$$

4. Continuous Wavelet Transform

The continuous wavelet transform is a wavelet transform where the dilation and translation parameters, named a and b in this case, vary continuously over R with $a \neq 0$ (Daubechies (1992)). Given the wavelet $\psi \in L^2(\mathrm{R})$ such that $\int \psi(t)dt = 0$ and a function $f \in L^2(\mathrm{R})$, the *Continuous Wavelet Transform (CWT)*, Tf, of $f(t)$, with $a \neq 0$ and $b \in$ R is defined by

[3]The remainder of dividing x by y is usually expressed as $x\, mod\, y$.

$$(Tf)(a,b) = |a|^{-1/2} \int dt f(t) \bar{\psi} \left(\frac{t-b}{a} \right). \tag{27}$$

The expression (27) computes the inner product in $L^2(\mathrm{R})$ of the function f against the family of functions, $\{\psi^{a,b}\}$, indexed by the parameters a, b, defined by

$$\psi^{a,b}(s) = |a|^{-1/2} \psi(\frac{s-b}{a}) \tag{28}$$

where $a \neq 0$ and $b \in \mathrm{R}$. The inner product is defined by $< f, g >= \int dt \bar{f}(t) g(t)$, where $\bar{f}(t)$ is the complex conjugate of $f(t)$.

When a changes and b remains fixed, $\psi^{a,b}(s) = |a|^{-1/2} \psi(\frac{s}{a})$ covers different frequency ranges. Changing the parameter b allows moving the location in time (x-axis or time-axis), every $\psi^{a,b}(s)$ is located around of $s = b$.

If $\psi \in L^2$ and that satisfies the following condition of admissibility

$$0 < C_\psi = 2\pi \int_{-\infty}^{\infty} d\xi |\xi|^{-1} |\widehat{\psi}(\xi)|^2 < \infty, \tag{29}$$

where $\widehat{\psi}$ is the Fourier transform of ψ (see eq. (1)), then the function f can be reconstructed from its CWT using the equation:

$$f = C_\psi^{-1} \int_{-\infty}^{\infty} \int_{-\infty}^{\infty} \frac{da \cdot db}{a^2} < f, \psi^{a,b} > \psi^{a,b}, \tag{30}$$

where $\psi^{a,b}(s) = |a|^{-1/2} \psi(\frac{s-b}{a})$, and $<,>$ denotes the inner product in L^2. The constraint (29) is satisfied if $\psi \in L^1(\mathrm{R})$ (i.e.: $\int |f(t)| dt < \infty$) and $\int \psi(x) dx = 0$ since under this assumption $\widehat{\psi}$ is continuous, then to get $C_\psi < \infty$ is sufficient that $\widehat{\psi}(0) = 0$, or equivalently, $\int \psi(x) dx = 0$.

As an example consider the Haar mother wavelet $\psi(x)$ given in equation (10). For $a > 0$ we have

$$\psi^{a,b}(x) = \frac{1}{\sqrt{|a|}} \left(-I_{[b, b+\frac{a}{2}]}(x) + I_{(b+\frac{a}{2}, b+a]}(x) \right),$$

and the CWT

$$(Tf)(a,b) = \frac{1}{\sqrt{|a|}} \left(\int_{b+\frac{a}{2}}^{b+a} f(t) dt - \int_{b}^{b+\frac{a}{2}} f(t) dt \right).$$

For $a < 0$ the CWT is developed in a similar way. In the context of CWTs, some of the most frequently used wavelet families are real and complex Morlet wavelet, real and complex Mexican hat wavelet, real and complex Shannon wavelet, among others.

The *Morlet Wavelet* or Gabor wavelet (Daubechies (1992)), is a continuous wavelet depending on parameter σ. Its Fourier transform, $\hat{\psi}$, is a displaced Gaussian, tuned somewhat so that $\hat{\psi}(0) = 0$,

$$\hat{\psi}(\xi) = \pi^{-\frac{1}{4}} \left(e^{-(\xi - \xi_0)^2/2} - e^{-(\xi^2 + \xi_0^2)/2} \right), \tag{31}$$

$$\psi(t) = \pi^{-\frac{1}{4}} \left(e^{-i\xi_0 t} - e^{-\xi_0^2/2} \right) e^{-\frac{t^2}{2}}, \tag{32}$$

where ξ_0 is often chosen as $\pi \left(\frac{2}{\ln(2)} \right)^{1/2} \simeq 5.336$ or $\xi_0 = 5$ for simplicity. The Morlet wavelet for $\xi_0 = 5$ is shown in Figure 6. This wavelet can be found in its complex version or in a real-valued version.

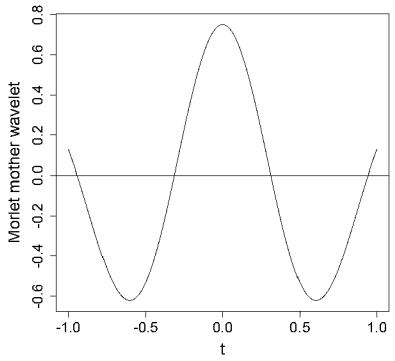

Figure 6. Morlet mother wavelet for $\xi = 5$ is shown in blue colour.

The Mexican hat wavelet or the Ricker wavelet is the second derivative of the Gaussian $e^{-x^2/2}$ and is defined by

$$\psi(x) = \frac{2}{\sqrt{3}} \pi^{-1/4} (1 - x^2) e^{-x^2/2}$$

after normalization to get $||\psi||_2 = 1$ (L^2(R)-norm) and $\psi(0) > 0$. Its plot is reminiscent of a cross section of a Mexican hat. The complex Mexican hat wavelet is formulated in terms of its Fourier transform given by $\hat{\psi}(\xi) = 2\sqrt{\frac{2}{3}} \pi^{-1/4} \xi^2 e^{-\frac{1}{2}\xi^2} I_{(0,+\infty)}(\xi)$.

The Fourier transform of the Shannon wavelet (Mallat (1998)) is the following:

$$\hat{\psi}(\xi) = \begin{cases} e^{-\frac{i\xi}{2}} & \text{if } \xi \in [-2\pi, -\pi] \cup [\pi, 2\pi] \\ 0 & \text{otherwise} \end{cases}$$

and the continuous wavelet is $\psi(x) = \frac{\sin(2\pi(t-1/2))}{2\pi(t-1/2)} - \frac{\sin(\pi(t-1/2))}{\pi(t-1/2)}$. This wavelet has infinite continuous derivatives with decay as $\frac{1}{t}$ at infinity due to the discontinuities of $\hat{\psi}(\xi)$ at $\xi = \pm\pi$ and $\xi = \pm 2\pi$.

4.1. Scalogram

The scalogram, a graph of the absolute value of the CWT, $|Tf|$, as a function of time, is used for different types of analysis. Color levels (high values of $|Tf|$ are in red) or gray levels are used (high values of $|Tf|$ are in black, zero in white) and a^{-1} is plotted on the ordered (y-axis). Some applications of the scalogram include

period detection in time series, change point detection, function discontinuity detection, signals recovering, among others. In all cases, the wavelet transform can detect the location in time of the event found.

The CWTs of 4 time series examples are shown below. They were done with the package Wavecomp in R [4] that uses Morlet wavelet family. In the scalogram, a range of colors appears related to the p-value obtained from a hypothesis test that is carried out via simulations:

H_0: There is no joint periodicity.

When H_0 is rejected, it indicates a great possibility that the periodicity is present in the data set. Given a level of significance, for example 0.01 or 0.05, the null hypothesis will be rejected if the p-value is smaller than the level of significance chosen. The scalogram shows the CWT values for each time and period in a range of colors from blue to red and a black contour line where the maximum values of the CWT are found for each instant of time. This black line, like the red regions, is found at the times and periods of highest wavelet power levels, where H_0 is rejected.

The first example is a sinusoidal data set with a period P=50. In Figure 7 you can see, from left to right, the original signal, the scalogram (with the period on the y-axis) and the reconstruction of the signal from the CWT. In this example 'Time' and 'Index' on the x-axis correspond to the step of time of the curve. In the middle panel, you can see that the CWT detects the period of 50 of the signal.

In Figure 8 the second example is showed: a signal with a variable period between $P = 20$ and $P = 100$. In this figure, from left to right, the original signal, the scalogram (with the period on the y-axis and the time step on the x-axis) and the reconstruction of the signal from the CWT can be seen. In the center panel of the figure, it is shown how the scalogram detects the variable period of the signal, its tendency and the reconstruction of the signal on the left panel is quite accurate. We can compare the performance of the scalogram with the STFT showed on the right panel of Figure 4.

In Figure 9, a signal with two periods: $P = 30$ and $P = 80$, both along all the range, is shown. In the figure, from left to right, the original signal, the scalogram (with the period on the y-axis and the time step called 'Index' on the x-axis) can be observed. On the right panel, it is easy to see two zones in red with a black line across indicating the two periods present in the signal.

Figure 10 shows a signal with two periods: $P = 30$ and $P = 80$, in separate intervals of time. On the right panel, it is simple to see two intervals of time with two different periods for the signal. The CWT can detect the instant of time when the change of period occurs.

In the four examples presented, some of the potentialities of the CWT can be observed: it can detect one or more periods present in the curve and indicate the time interval in which the detected period influences the behavior of the time series as well as it can detect the points of change where the change between

[4] https://cran.r-project.org/web/packages/WaveletComp/WaveletComp.pdf

periods occurs. All of these are regarding an evenly sampled time series. Because of this, for 55 Cyg light curve (from TESS mission) a partition of the data is made and they are analyzed separately obtaining the scalograms in Figure 12. Although each partition still has irregularly sampled data, the time differences between the measurements are quite similar allowing the use of the Wavecomp package which is for equidistant time series.
Figure 12 shows two significant periods (solid black lines). A first period p_1 that starts with a value $2 \leq p_1 \leq 4$, grows in time and stands at $p <\approx 4$ at the end of the time interval (right panel); and a local in time period $p = 2$ that appears during the middle time of the first part of the data (middle panel) and decreases to a value just below 2 during the second part (right panel).

The graph is seen divided into two regions, one with brighter colours and the other with fainter colours. It corresponds to the cone of influence, described in Lenoir & Crucifix (2018), the wavelet analysis extends a little at the edges of the time series, due to the wavelet support (values where the wavelet is not null) then a part goes beyond after the last point of the time series, or before the first point of the time series. Due to this, one half cone is removed from the left end and another from the right end, from the area under analysis, producing the region with fainter colors. This situation is present in each of the plots but is more evident in this figure.

For data with time differences between more irregular measurements it is recommended to look for other alternatives. Some of them are listed below. Developments have been made by interpolating the data to obtain equispaced data (see for instance Thiebaut & Roques (2005)) or in other cases the continuous wavelet transform has been used on the raw data (Lenoir & Crucifix (2018)). Foster (1996) proposed the use of the weighted wavelet Z transform to face this problem. In his work the author proposed an adaptation of wavelet analysis for irregularly spaced data called Weighted Wavelet Z transform (WWZ-transform). It consists of analyzing the data through projections of the Morlet mother wavelet, which add up with some specific weighting. Foster (1996) showed the efficiency of the method in some signals although its limitation consists in detecting periods and amplitudes when the gap in data is larger than the period to be detected. WWZ transform proved good performance discerning in frequency and time, period and amplitude of long-period stars in presence of unevenly data.

According to Lenoir & Crucifix (2018), interpolation procedures can significantly affect the results especially when hypothesis testing is used. The authors proposed a method to analyzed unevenly time series by means of the scalogram of wavelet analysis without interpolation of the data. The authors proposed to use projections of the continuous Morlet mother wavelet, without weighting, and implemented his methodology in the WEAVEPAL software (developed on Python 2, Lenoir & Crucifix (2017)). The method seems efficient as long as the length of the intervals without observations is little variable. It is also observed as a limitation the inability to detect periods when the gap is larger than the period to be detected.

Tarnopolski et al. (2020) argue that irregular data makes it difficult to calculate certain magnitudes and introduces spurious peaks in the power spectral

density. To solve this problem the authors propose to interpolate the data to make them regular using a method based on the ARMA time series model called MIARMA.

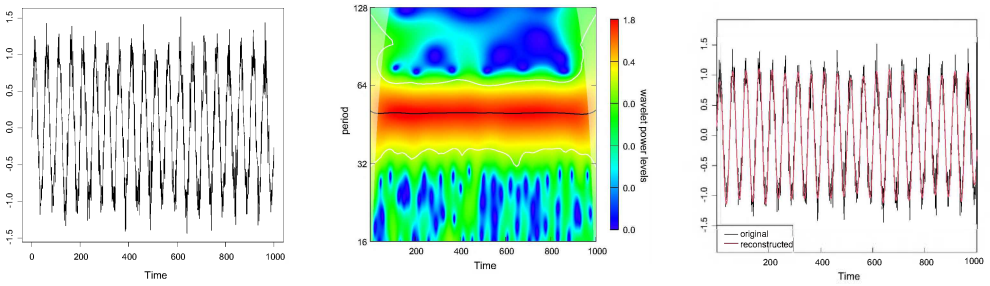

Figure 7. The original sinusoidal signal with period 50, the scalogram and the reconstruction from the CWT are shown from left to right panels.

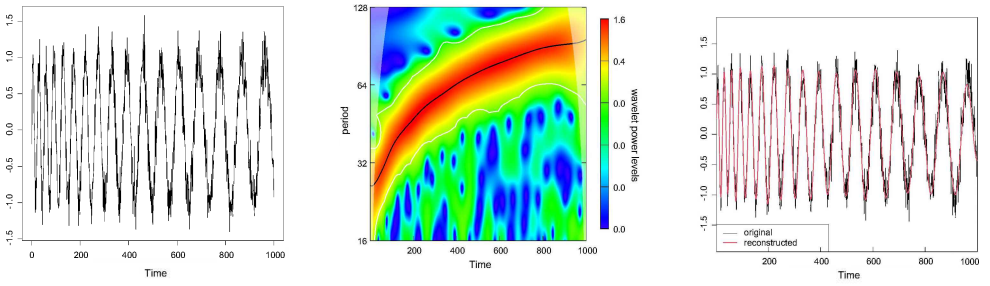

Figure 8. The original sinusoidal signal with a variable period from 20 to 100, the scalogram and the reconstruction from the CWT are shown from left to right panels. Center panel shows how the scalogram manages to capture the variable period.

5. Conclusions

In this paper we presented a brief summary of the theory of wavelet analysis, multiresolution analysis, and the continuous wavelet transform along with some applications in periodic time series to detect periods or points of change through simulations and real data. The R software was used for the implementation of numerical simulations and the wavelet analysis.

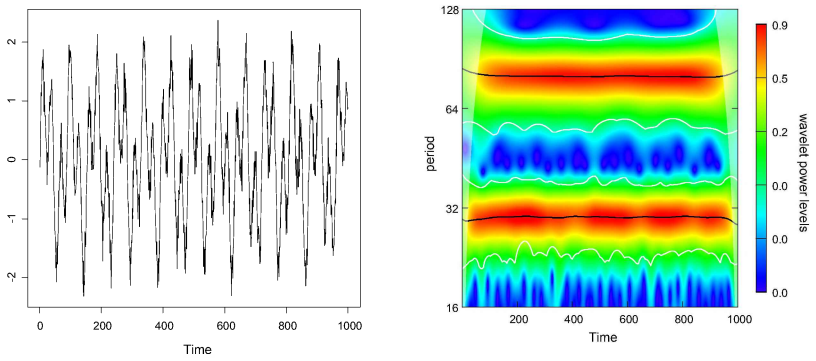

Figure 9. The original sinusoidal signal with two periods $(30, 80)$ along the curve is shown on the left panel. The corresponding scalogram with the evidence of the two periods along all the range of the signal is shown on the right panel.

6. R Codes

Some of the R codes used in this Chapter are presented in this section. Note that the '+' sign is used in some commands to indicate that they continue on the next line. When running them in R you must select all the lines corresponding to the command, deleting the '+'. For example, for the command:

```
plot(t,haar3, type='l', ylim=c(-2.1,2.1),xlim=c(-0.5,2.5),
+                 col='blue')
```

put in R without '+' and select all the sentences in order to run it:

```
plot(t,haar3, type='l', ylim=c(-2.1,2.1),xlim=c(-0.5,2.5), col='blue')
```

6.1. STFT

Figure 1:

```
install.packages('e1071')
library(e1071)

t1<-seq(0,100,0.01)
length(t1)
x1<-sin((0.2*pi)*t1[1:3000])
x2<-1.5*sin(0.5*pi*t1[3001:4000])
x3<-2*sin((0.8*pi)*t1[4001:10001])
x<-c(x1,x2,x3)
z1<-sin((3/5)*t1[1:3000])
z2<-0.5*sin(0.5*t1[3001:6000])
z3<-2*sin((1/10)*t1[6001:10001])
obj<-c(z1,z2,z3)
```

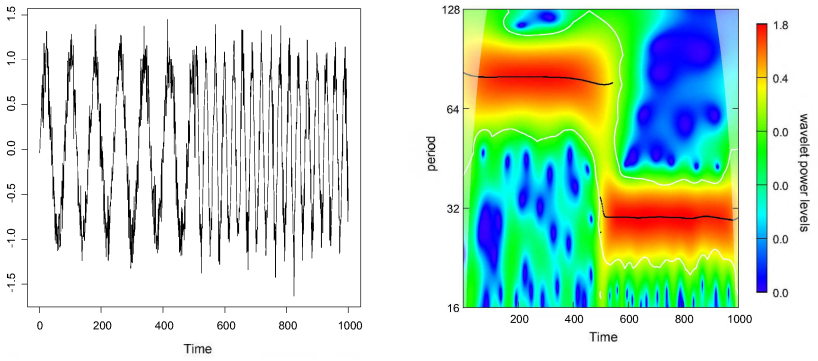

Figure 10. The original sinusoidal signal with two periods, $P = 80$ for the first part of the curve and $P = 30$ for the final part is shown on the left panel. The corresponding scalogram with the evidence of the two detected periods and the time interval involving each one is shown on the right panel.

```
par(mfrow=c(2,2))
plot(x, type='l', main='Sine wave 1', xlab='Time', ylab='Signal')
y<-e1071::stft(x)
plot(y, xlab='', ylab='', main='STFT of Sine wave 1', ylim=c(0,15))
plot(obj, main='Sine wave 2', xlab='Time', ylab='Signal',type='lines')
z<-e1071::stft(obj)
plot(z, xlab='', ylab='', main='STFT of Sine wave 2', ylim=c(0,15))
```

Figure 2:

```
install.packages('lomb') #Lomb Scargle periodogram
library(lomb)
lsp(x, times=t1,ofac=5, xlim=c(0,0.5))
```

Figure 3:

```
install.packages('e1071')
library(e1071)

x<-rnorm(500)
y<-e1071::stft(x)
obj<-arima.sim(n = 63, list(ar = c(0.8897, -0.4858), ma = c(-0.2279, 0.2488)),
+                  sd = sqrt(0.1796))
```

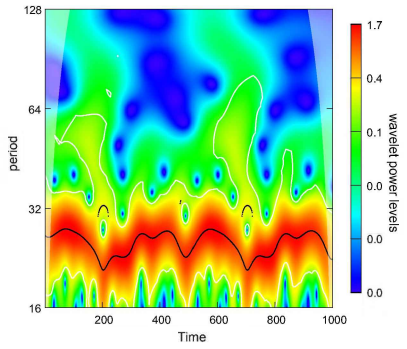

Figure 11. The scalogram of the same sinusoidal curve of Figure 7 with period 50 where 50% of data was removed. In presence of irregular sampled data the scalogram underestimates the period.

```
z<-e1071::stft(obj)


plot(x, type='l', main='White noise', xlab='Time', ylab='Signal')
plot(y, xlab='', ylab='', main='STFT of white noise')
plot(obj, main='ARMA(2,2)', xlab='Time', ylab='Signal')
plot(z, xlab='', ylab='', main='STFT of ARMA(2,2)')
```

Figure 4:

```
install.packages('WaveletComp')
library(WaveletComp)

w = periodic.series(start.period = 20, end.period = 100, length = 1000)
w = w + 0.2*rnorm(1000)
wy<-e1071::stft(w)

par(mfrow=c(1,2))
plot(w, type='l', main='A signal with variable periods', xlab='Time', ylab='Signal')
plot(wy, xlab='', ylab='', main='STFT of the signal', ylim=c(0,20))
```

6.2. Haar Wavelet

Figure 5:

```
t<-seq(-2,3,0.01)
length(t)
```

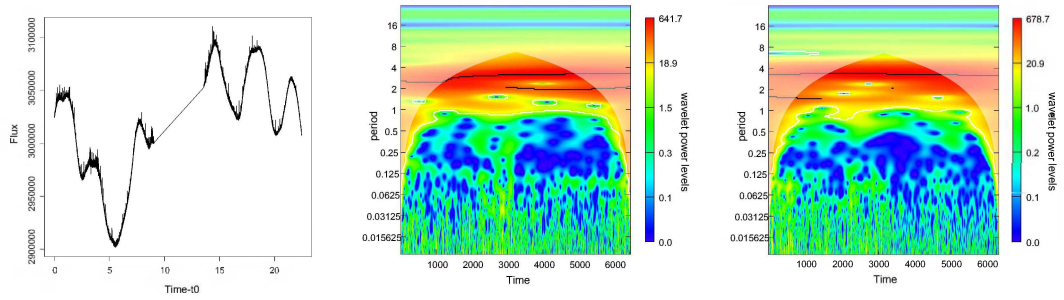

Figure 12. The original light curve of 55 Cyg is shown on the left panel. After splitting the signal in two parts the two corresponding scalograms are shown on the right panels.

```
par(mfrow=c(2,3))
title('Wavelet Haar')
#Plot 1: Wavelet Haar father: j=0 k=0. -----------------ORIGINAL
haar1<-c(rep(0,200), rep(1,100), rep(0,201))
plot(t,haar1, type='l', ylim=c(-2.1,2.1),xlim=c(-0.5,2.5), col='blue',
+              ylab='', xlab='(a)')
abline(v=0)
abline(h=0)

#Plot 2: Wavelet Haar father: j=0 k=1
haar2<-c(rep(0,300), rep(1,100), rep(0,101))
plot(t,haar2, type='l', ylim=c(-2.1,2.1),xlim=c(-0.5,2.5), col='blue',
+              ylab='', xlab='(b)')
abline(v=0)
abline(h=0)

#Plot 3: Wavelet Haar father: j=1 k=1/2
haar3<-c(rep(0,250), rep(2,25), rep(0,226))
plot(t,haar3, type='l', ylim=c(-2.1,2.1),xlim=c(-0.5,2.5), col='blue',
+               ylab='', xlab='(c)')
abline(v=0)
abline(h=0)

#Plot 4: Wavelet Haar mather: j=0 k=0.  ---------------ORIGINAL
haar4<-c(rep(0,200), rep(1,50), rep(-1,50),rep(0,201))
plot(t,haar4, type='l', ylim=c(-2.1,2.1),xlim=c(-0.5,2.5), col='violet',
+              ylab='', xlab='(d)')
abline(v=0)
abline(h=0)

#Plot 5: Wavelet Haar mather: j=0 k=1
haar5<-c(rep(0,300), rep(1,50), rep(-1,50),rep(0,101))
```

```
plot(t,haar5, type='l', ylim=c(-2.1,2.1),xlim=c(-0.5,2.5), col='violet',
+             ylab='', xlab='(e)')
abline(v=0)
abline(h=0)

#Plot 6: Wavelet Haar mather: j=1 k=1
haar6<-c(rep(0,300), rep(2,25), rep(-2,25),rep(0,151))
plot(t,haar6, type='l', ylim=c(-2.1,2.1),xlim=c(-0.5,2.5), col='violet',
+              ylab='', xlab='(f)')
abline(v=0)
abline(h=0)
```

6.3. CWT and Scalogram

This section is based on Roesch & Schmidbauer (2018).

Figure 7: A series with a constant period, period equal 50

```
install.packages('WaveletComp')
library(WaveletComp)

set.seed(1)
x1 = periodic.series(start.period = 50, length = 1000)
x1 = x1 + 0.2*rnorm(1000)  # add some noise
plot(x1, type='l', xlab='Time')
date=1:1000

my.data <- data.frame(date=date, x = x1)
my.w <- analyze.wavelet(my.data, "x",
loess.span = 0,
dt = 1, dj = 1/250,
lowerPeriod = 16,
upperPeriod = 128,
make.pval = TRUE, n.sim = 10)
#scalogram
wt.image(my.w, color.key = "quantile", n.levels = 250,
legend.params = list(lab = "wavelet power levels", mar = 4.7))
#red zones with black lines corresponds to more significant periods


#recover the significant periods and the average period
ta<-my.w$Period[which(my.w$Ridge==1,arr.ind = TRUE)[,1]]
mean(ta)

#reconstruct the signal using wavelets
reconstruct(my.w, plot.waves = FALSE, lwd = c(1,2),
legend.coords = "bottomleft", ylim = c(-1.8, 1.8))
```

Figure 8: A series with a variable period.

```
install.packages('WaveletComp')
library(WaveletComp)

x = periodic.series(start.period = 20, end.period = 100, length = 1000)
x = x + 0.2*rnorm(1000)
plot(x1, type='l', xlab='Time')

my.data <- data.frame(x = x)
my.w <- analyze.wavelet(my.data, "x",
loess.span = 0,
dt = 1, dj = 1/250,
lowerPeriod = 16,
upperPeriod = 128,
make.pval = TRUE, n.sim = 10)
wt.image(my.w, n.levels = 250,
legend.params = list(lab = "wavelet power levels"))
#The variable period is observed in the scalogram

#reconstruction
my.rec <- reconstruct(my.w)
```

Figure 9: A series with two periods.

```
install.packages('WaveletComp')
library(WaveletComp)

set.seed(1)
x1 <- periodic.series(start.period = 80, length = 1000)
x2 <- periodic.series(start.period = 30, length = 1000)
x <- x1 + x2 + 0.2*rnorm(1000)
plot(x, type='l', xlab='Time')


my.data <- data.frame(x = x)
my.w <- analyze.wavelet(my.data, "x",
loess.span = 0,
dt = 1, dj = 1/250,
lowerPeriod = 16,
upperPeriod = 128,
make.pval = TRUE, n.sim = 10)
wt.image(my.w, n.levels = 250,
legend.params = list(lab = "wavelet power levels") )

#reconstruction
reconstruct(my.w, plot.waves = TRUE, lwd = c(1,2),
legend.coords = "bottomleft")
```

Figure 10: A series with two periods in different times.

```
install.packages('WaveletComp')
library(WaveletComp)

set.seed(1)
x1 <- periodic.series(start.period = 80, length = 1000)
x2 <- periodic.series(start.period = 30, length = 1000)
x <- c(x1 , x2) + 0.2*rnorm(1000)
plot(x, type='l', xlab='Time')


my.data <- data.frame(x = x)
my.w <- analyze.wavelet(my.data, "x",
loess.span = 0,
dt = 1, dj = 1/250,
lowerPeriod = 16,
upperPeriod = 128,
make.pval = TRUE, n.sim = 10)
wt.image(my.w, n.levels = 250,
legend.params = list(lab = "wavelet power levels") )
```

Figure 11: An unevenly sampled data.

```
install.packages('WaveletComp')
library(WaveletComp)

set.seed(1)
x1 = periodic.series(start.period = 50, length = 1000)
x1 = x1 + 0.2*rnorm(1000)  # add some noise
date=1:1000


#Deleting some data to produce gaps
obs <- sample(seq(x1), 0.5*length(x1)) # 50% gaps
x11 <- x1[sort(obs)]
date1 <- date[sort(obs)]

par(mfrow=c(1,2))
plot(x1 ~ date, pch=".", cex=2)
plot(x11 ~ date1, pch=".", cex=2)

par(mfrow=c(1,1))

my.data11 <- data.frame(date=date1, x = x11)   #with unevenly data
my.w11 <- analyze.wavelet(my.data11, "x",
loess.span = 0,
```

```
dt = 1, dj = 1/250,
lowerPeriod = 16,
upperPeriod = 128,
make.pval = TRUE, n.sim = 10)

wt.image(my.w11, color.key = "quantile", n.levels = 250,
legend.params = list(lab = "wavelet power levels", mar = 4.7))
#In presence of unevenly data wavecomp subestime the period.

reconstruct(my.w11, plot.waves = FALSE, lwd = c(1,2),
legend.coords = "bottomleft", ylim = c(-1.8, 1.8))
#Be carefull, Wavecomp analyze the serie sticking the gaps
```

7. Notation

Some notation used in the article is the following:

R is the set of real numbers,

Z is the set of integer numbers,

$\oplus$ direct sum of two or more linear sub-spaces, that is, a new subspace spanned for generators of each sub-space in the direct sum where each is orthogonal to any other.

$\ominus$ of a subspace included in another subspace, if $B \subset A$, then $A \ominus B$ is the orthogonal complement of B within A,

$||.||_2$ 2-norm of functions, $||.||_2 = \int_{-\infty}^{\infty} |f(t)|^2 dt$,

$L^2(\mathrm{R})$ Hilbert space of real functions with finite 2-norm.

Acknowledgments. This project has received funding from the European Union's Framework Programme for Research and Innovation Horizon 2020 (2014-2020) under the Marie Skłodowska-Curie Grant Agreement No. 823734.

References

Beylkin G., R. C., V. R., 1991, *Comm. Pure and Appl. Math.*, **44**, 141
Cáceres G. A. e. a., 2019, *Astron. J.*, 158(57)
Daubechies I., 1988, *Comm. Pure and Appl. Math.*, **41**, 909
Daubechies I., 1992, *Ten Lectures on Wavelets*, Society for Industrial and Applied Mathematics
Eyheramendy S., Elorrieta F., Palma W., 2018, *MNRAS*, **481(4)**, 4311
Fischer-Cripps A., 2002, *"Newnes Interfacing Companion", A. Fischer-Cripps (ed.)*, Newnes, Oxford
Foster G., 1996, *AJ*, **112**, 1709
Härdle W., Kerkyacharian G., Picard D., Tsybakov A., 1998, *Wavelets, approximation, and statistical applications*, Springer-Verlag, New York

Kelly B. C., C. B. A., M. S., A. S., P. U., 2014, *ApJ*, **788(1)**, 33
Lenoir G., Crucifix M., 2017, *EGU General Assembly Conference Abstracts*, EGU General Assembly Conference Abstracts, p. 15162
Lenoir G., Crucifix M., 2018, *Nonlin. Processes Geophys.*, **25**, 175
Mallat S., 1989, *IEEE Transactions on Pattern Analysis and Machine Intelligence*, **11**, 674
Mallat S., 1998, *A Wavelet tour of signal processing*, Academic Press, Elsevier, United States, 1998
Meyer Y., 1986, *Lectures given at the University of Torino, Italy*, pp 1–42
Percibal D. B., Walden A. T., 2000, *Wavelet Methods for Time Series Analysis*, Cambridge University Press
Poularikas A., 2010, *The Transforms and Applications Handbook. 3rd Edition*, Taylor and Francis Group, LLC
Roesch A., Schmidbauer H., 2018, *WaveletComp: Computational Wavelet Analysis*, R package version 1.1
Tarnopolski M., Åżywucka N., Marchenko V., Pascual-Granado J., 2020, *The Astrophysical Journal Supplement Series*, **250(1)**, 1
Thiebaut C., Roques S., 2005, *EURASIP Journal on Applied Signal Processing*, **2005**, 852587